STRUCTURAL DEFORMATION CAUSED BY AERODYNAMIC EXCITATIONS DURING THE PASSING OF MAGLEV VEHICLES

Sandro Monaco[*] and Florian Dignath[†]

[*]Dipartimento di Ingegneria Meccanica
Politecnico di Milano, Campus Bovisa, Via La Masa 34, 20156 Milano, Italy
e-mail: Sandro.Monaco(at)gmail.com,

[†]Basic Technologies
ThyssenKrupp Transrapid, Moosacher Str. 58, 80809 München, Germany
e-mails: Florian.Dignath(at)thyssenkrupp.com

Keywords: Transrapid, Passing of Vehicles, Pressure Wave, Structural Vibrations, Finite Elements, Transient Analysis.

1   INTRODUCTION

The Maglev vehicle Transrapid is the first fundamental innovation in railroad engineering since the construction of the first railroads. It is the world's only commercially-available high speed Maglev technology. As a result of over 25 years of continuous design, testing and refinement, the Transrapid Maglev technology is the first of such a transportation system approved for public use. The superspeed maglev system has no wheels, axles, transmissions, or pantographs. It hovers instead of rolling without any contact with the guideway. Instead of wheels and rails, the Transrapid uses non-contact electromagnetic levitation, guidance, and propulsion systems -wear-free electronics instead of mechanical components and achieves a routine operating speed of up to 500 kilometers per hour. An overview of the design of the vehicle and guideway is given in [5] and a detailed comparison between the system properties of the Transrapid and the system properties of conventional high-speed trains can be found in [6].

The first commercial application is the airport link of Shanghai from the financial centre to the 30 km-distant Pudong International airport. The commercial service started in January 2004. On this line the Transrapid accelerates to a speed of up to 450 km/h traveling on a 30 km double-track guideway. The dependable total journey time of 7.5 minutes is a significant improvement with respect to traditional airport links (car, bus) with a travel time of at least 45 minutes. The Maglev fleet consists of three Transrapid vehicles each consisting of five sections. Up to now, over ten million passengers have glided to or from the airport.

Fig. 1: Maglev vehicle Transrapid in Shanghai: Two vehicles passing each other at a relative speed up to 1 000 km/h (image: Transrapid International)

1.1   Background of Aerodynamic Analysis

In recent years, with increasing traveling speed of the rail systems, aerodynamic load problems became very important. From the system point of view, aerodynamical topics which affect and define the interface between rolling stock, infrastructure and operation are of paramount importance and the corresponding loads increase with the vehicle speed.

If fast motor vehicles and trains pass in close proximity to each other, see Fig. 1, or move close to fixed objects such as barriers or buildings, the aerodynamic interactions can produce significant loads on the vehicle or the fixed object [4]. The magnitude and duration of the load depends on the velocity and geometry of the vehicles and also on the ambient wind speed and direction.

For high speed railways several studies have examined the loads produced by passing trains and their potential for causing an accident ([2]). Computational fluid dynamics (CFD) were used, e.g. to simulate a high speed passenger train passing a fixed object such as noise barriers or other trains at closing speeds of up to 350 km/h. The results of these studies show an important pressure load acting on the object which can have seri-

ous consequences. The experiments were carried out on conventional railway vehicles but from the system point of view, in principle, the aerodynamics of a maglev and a high-speed railway system do not differ. Although the safety aspect does not concern the Maglev vehicle Transrapid as strongly as it concerns conventional railways, because the Transrapid is guided by magnets on both sides and cannot derail, many aspects are similar. In both cases, the interaction of vehicles and infrastructure implies aerodynamic system issues, e.g. that of train induced aerodynamic loads leading to structural vibrations and a decrease of ride comfort. Specific aspects of the maglev system – e.g. aerodynamic interaction between vehicle and guideway – had been early addressed and extensively investigated also by full-scale tests.

2   AERODYNAMIC EXCITATION DURING THE PASSING OF TWO VEHICLES

The pressure load caused by passing maglev vehicles has an important aerodynamic effect on the sidewall motion and therefore on the ride comfort [7]. While two vehicles are passing each other at high relative speed, the quasi-static pressure distribution along each vehicle presents a dynamic load on the other vehicle. Especially the vehicle bow area and the vehicle tail area each produce a pressure pulse on the side of the other vehicle. The high and low pressure zones around the bow area of the oncoming vehicle present a dynamic load on the structure of the vehicle considered and lead to structural oscillations of the carriage side wall. The amplitude of the structural response increases as it runs along each carriage side wall to the end of each carriage. Then it starts with a small amplitude at the next carriage wall because the carriages are structurally decoupled at each section end.

This vehicle-induced dynamic pressure load (Fig. 2) strongly depends on the velocity of the oncoming vehicle, the geometry of the bow-part of the oncoming vehicle and the distance between the two tracks. The time behavior is given by the relative velocity between the two vehicles. The most important aspect is that this load generates a traveling wave along the side structure of the carriage body. This kind of load leads to strong vibrations if it excites a structural mode of the carriage body. This can lead to deformations which are significantly greater than static deformations at the same pressure load. Structural stresses and reduced life time could be a consequence.

In order to analyze the dependency of the structural deformations on the parameters of the vehicle and its operation, transient FE-computations are conducted within the work of a Master Thesis [3].
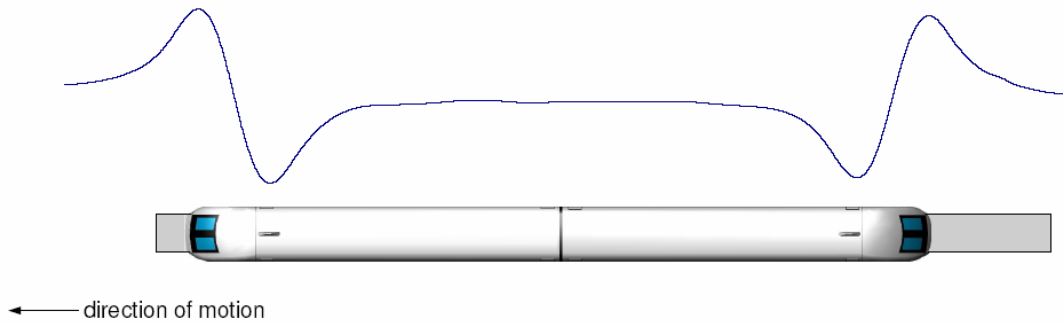
← direction of motion

Fig. 2: Shape of vehicle-induced dynamic pressure load.

2.1 Measurements

In order to analyze the pressure load caused by the passing of two vehicles and verify the structural load of the vehicle, a field measurement testing was conducted with maximum speed of 430 km/h on November 2003 in Shanghai. The field measurements were performed at different conditions and passing speed of Maglev vehicles. Therefore it was possible to take measurements of the pressure acting on the vehicle and the displacements of the structure.

Two maglev vehicles were used in the testing, Fig. 3. One is a five-section-vehicle, called PV2, the other is a three-section-vehicle, called PV1. For the investigation of the outer pressure load, pressure sensors have been installed on defined measuring points on PV2. The pressure load working on PV2 has been measured at different relative speeds.

For the investigation of the deformation of the structure a displacement sensor was fixed on one side at the first window (next to the bow) and on the other side on the floor of the carriage body.
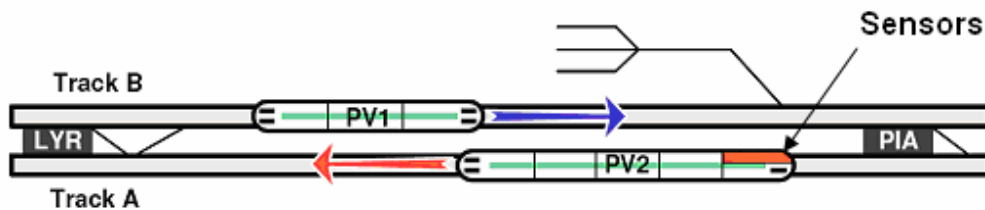

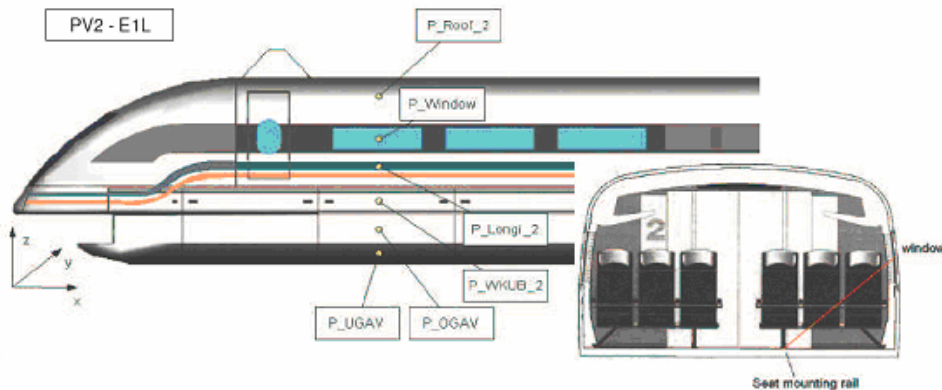**Fig. 3:** Test configuration of flying-passing situation

Fig. 4: Pressure and displacement measurements points on the vehicle

2.1.1. Measured Pressure Wave

Analyzing the pressure signal (Fig. 5), it can be seen that the pressure loads on PV2 increase quickly from a low value (~0), which depends on the running velocity of PV2 and natural wind environment, to a peak, P_{MAX}, when PV1 is approaching and its bow reaches PV2. Then a fast pressure decrease to a negative peak, P_{MIN}, follows while the bow passes. The pressure level at the cylindrical part of the vehicle returns almost to zero and at the end of PV1 a negative peak is followed by a positive as the tail of the oncoming vehicle is passing. The pressure fluctuation after the passing vehicle can be explained by the presence of turbulences within the vortex trailing.
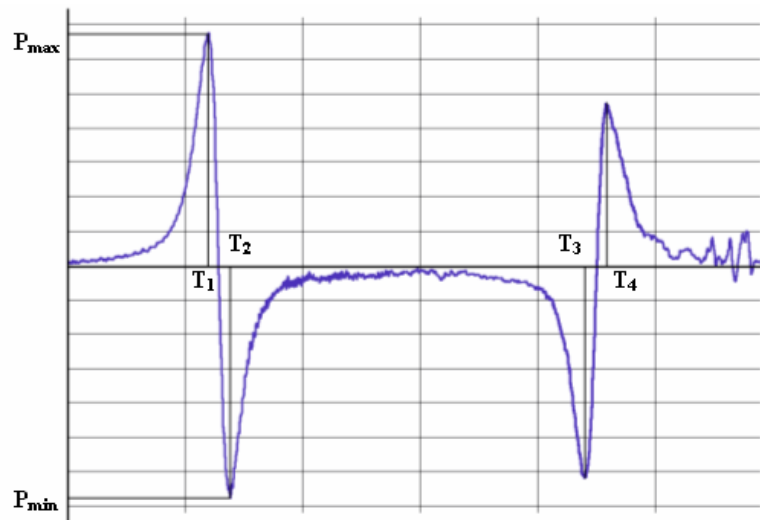

Fig. 5: Exemplary measurement of pressure wave

2.1.2. Measured Deformation

Deformations were measured with the sensor connected to the center of the first window behind the bow. As shown in Fig. 6 the signal of the displacement of the window has great similarities to the pressure wave. When the positive pressure peak appears, the window is compressed and the sensor shows a negative displacement. This is followed by a positive displacement which corresponds to a negative pressure on the outer surface. These displacement measurements can directly be compared to the computation results of the FE simulations.
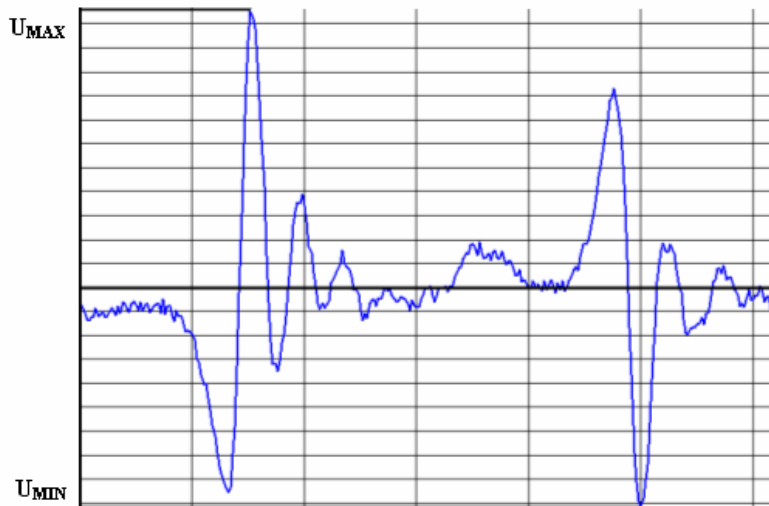
Fig. 6: Exemplary measurement of displacement on carriage body

2.2   Discussion of Aerodynamic Excitation

From these measurements it is possible to conclude that the traveling pressure wave excites structural vibrations of the carriage side wall. The amplitudes of the structural vibrations can be several times larger than the static deformations if the velocity of the pressure wave corresponds to an Eigenmode of the carriage body. Structural stresses and a decreased life time of the structure could be consequences.

Regarding these measurements, some considerations are possible:

1) The pressure wave has a form which depends on the relative speed and the form of bow and tail of the vehicle.
2) The maximal peak is approximately proportional to the square of the running speed of the oncoming vehicle only.
3) Below 200 km/h the maximal peak is smaller than 250 Pa and has a negligible influence on the body cell.
4) The spatial form of the wave does not depend on the traveling speed. The peak to peak distance of the bow caused pressure wave is about 4.6 m
5) The amplitude of the wave is nearly constant up to the end of the side window, while it decreases towards the roof according to the growing distance between the two vehicles. The reduction is about 30% at the start of the actual roof, where the distance between the two vehicles is increased by about 50-60 cm.
6) The time distance between bow and tail effect depends on the relative speed and the oncoming vehicle's length. The side wall of the passing vehicle generates a modest negative pressure during passing.
7) For the simulation only the bow effect is used because of its clearer signal and its pressure value. The tail effect can be simulated using the same function as for the bow, but reduced and inverted.

3   FINITE ELEMENT MODEL OF THE TRANSRAPID CARRIAGE

In the following, the design of the Transrapid carriage is described before deriving a suitable Finite Element model for the transient analysis.

3.1   Design of the Transrapid Carriage

The maglev vehicle Transrapid TR08 has a lightweight carriage body consisting of three main components, bow, carriage body cell and sub-floor structure, as shown by Lobach [1]. The carriage body is manufactured in hybrid-building-method. The sub-floor structure supports the carriage body cell and houses the sub-floor facilities as well as signal and power cables. In this part of the carriage the distinctive elements of a maglev vehicle are housed: the electrical components for the control of the magnets and the power supply. An important aspect of the design of the Transrapid is the lightweight construction principle. The entire structure has to be as light as possible but at the same time stiff enough to support the loads acting on the structure by high-speed traveling. The lightness is fundamental for a high-speed transportation system because the necessary propulsion power is proportional to the weight. In order to reach a low weight the whole body consists of aluminum profiles and composite sandwich structures.

The sidewall and roof panels of the carriage body are made of aluminum composites with PEI-foam as core material covered with aluminum sheets at both sides. To connect the composite structures or sheets extruded aluminum profile, with different forms are applied. At both sides of the carriage body glass windows are applied and between the windows there is an aluminum post. Further structures which reinforce the sidewall are the door posts which are situated in the front and back of the carriage body. These posts are made of aluminum plates and are situated at a distance of approximately 18 m from each other. An accurate reproduction of this structure is fundamental for the analysis of the deformations caused by the pressure wave acting on the carriage body cell.
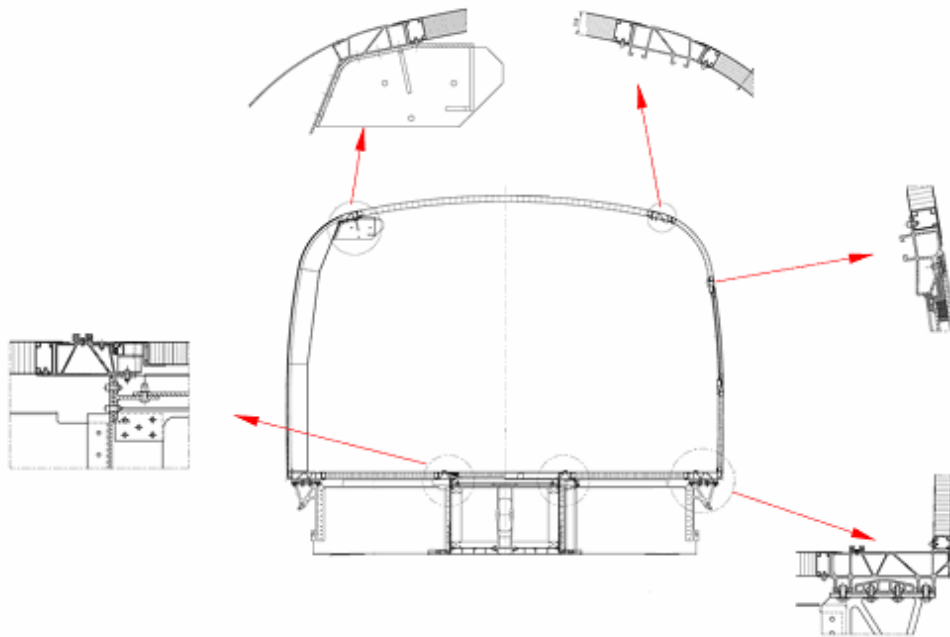
Fig. 7: Cross section with details of aluminum profiles

3.2   Finite Element Model

Since the geometry of the carriage body is characterized by thin sandwich walls with large surfaces an important aspect of the presented work is the creation of an efficient FE-Model which allows the computation of dynamic transient calculations, see Fig. 8. In order to obtain an efficient and at the same time accurate FE-Model a detailed analysis of each single part and module was executed. A combination of shell elements with layered 3D volume elements was developed in order to use the advantages of 2D-modelling of thin sheets with 3D-structural properties of sandwich structures and aluminum profiles.
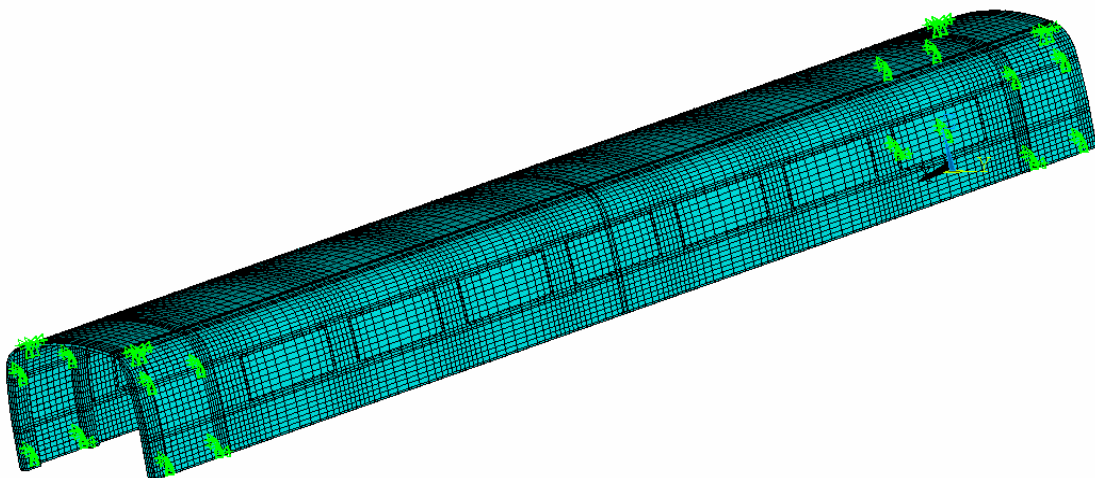

Fig. 8: Complete FE model of the carriage body of Transrapid TR08

Once the model was created it was necessary to validate it by comparison with experimental measurements on the real object. The first important step was the validation of the stiffness. For the Transrapid TR08 measurements of the carriage deformation recorded during a pressure-tightness test were available [8]. These data, regarding the deformations of the carriage body caused by application of a uniform pressure on the entire structure, were compared with the results of the FE model loaded with the same pressure. The comparison shown in Fig. 9 demonstrates the validation of the overall stiffness of the created model.

For a transient analysis, next to the stiffness also the inertia and the Eigenmodes of the structure are fundamental. From the technical reports of the Transrapid TR08 it is possible to see that parts of interior equipment, comprising side panels, roof panels, cable channel and some secondary electrical line are fixed to the carriage body structure. Their mass needs to be considered in order to model the overall inertia, while they do not contribute to the carriage stiffness. These elements are considered to be distributed homogeneous to the surrounding structure by an increase of the density of the materials of the sidewall and the roof, respectively, around each mass. As result of this operation the overall weight as well as the Eigenmodes of the structure were reproduced.

The resulting FE model possesses 28 000 elements and 141 000 degrees of freedom which is a significant reduction in comparison to the 540 000 degrees of freedom of the full model created directly from CAD data. It allows a full transient analysis of a complete carriage body loaded by the pressure wave within one hour of computation time using a PC with dual Pentium D, 3 GHz processor. As an example, the deformation at a specific time point is shown together with the FE-model in Fig. 10.
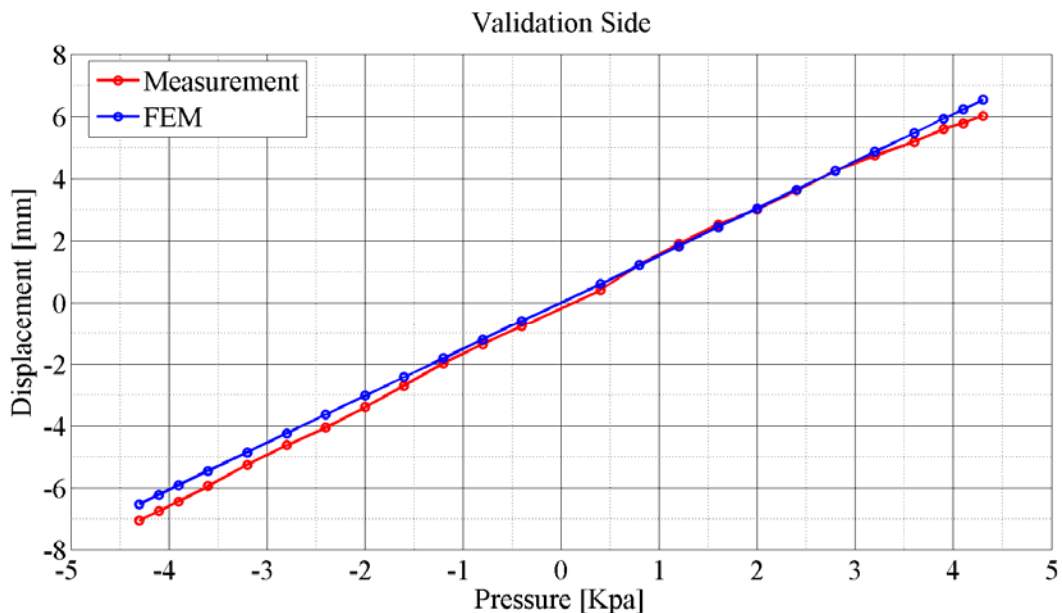

Fig. 9: Pressure-tightness measurements on Transrapid TR08 and FE model
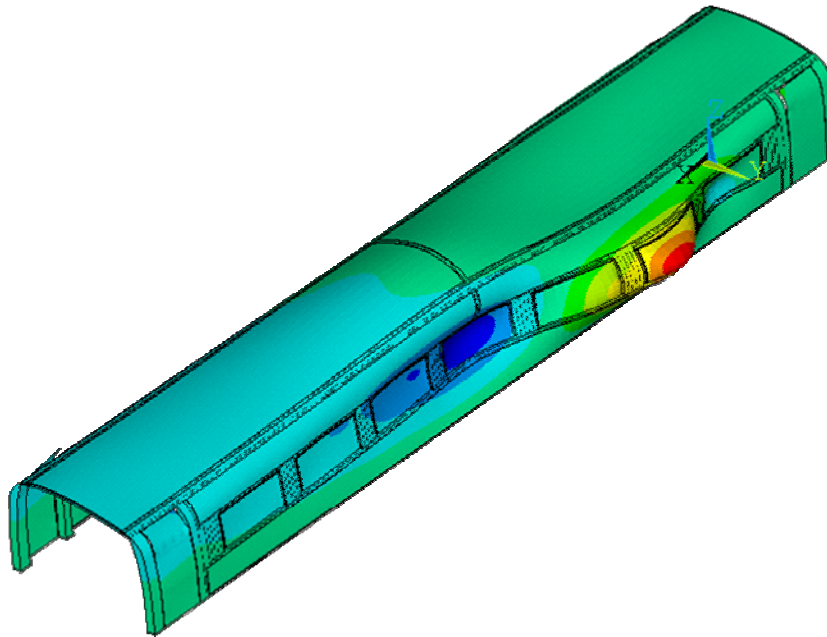
Fig. 10: FE-model of the carriage body. Deformation (shown exaggerated) caused by the pressure wave at one instance of the transient analysis

4   TRANSIENT ANALYSIS

The transient analysis on the carriage body is fundamental for the investigation of the dynamic effects which take place during the passing situation.

In order to analyze the interaction between the traveling pressure wave and the structural vibration of the carriage body, a full transient analysis is carried out. In order to specify the load as a function over time the load-versus-time curve is divided into suitable load steps. For the traveling pressure wave the load-steps were defined for different discrete positions of the wave along the side wall. As initial conditions both, initial displacements and initial velocities of the nodes, were assumed to be zero. The spatial form of the pressure wave, given from the measurements, was reproduced along the side wall and with decreasing amplitude along the curved part of the roof.

With this operation it was possible to define a discrete number of load steps which were maintained during all following simulations. Different traveling speeds were simulated by changing the time interval between the steps. So it is possible to have the same load step number for each simulation, which simplifies the comparison of the results.

Fig. 12 shows the maximal amplitudes along the sidewall taken from the transient analysis of the passing of the bow induced pressure wave. It can be seen that the maximal deformation occurs near the end of the carriage body. In order to validate the model this maximal deformation is compared to the deformation in the measurements at different velocities for 0-430 km/h [see Fig. 11]. The measured vehicle is standing at $v=0$ in these situations.

For a better comprehension of the problem further traveling velocities of the wave were simulated. For all simulated speeds the vehicle which generates the pressure wave

is assumed to be traveling at 430 km/h while the modeled vehicle, on which deformations have been measured, varies its velocity yielding the desired relative speed. This situation was set-up to keep the shape and the amplitude of the pressure wave constant for all simulations. The difference in the resulting deformation therefore is due to the different relative velocities only. As reference for the deformation values a quasi static simulation, with the traveling wave passing along the sidewall at 2 km/h, was conducted. The deformations resulting from this simulation represent the static deformation caused by the pressure wave where no dynamic effect is observable.

Considering the deformations taken along the sidewall just under the side windows, as shown in Fig. 12, and comparing the factor between the deformations at the given relative velocity with the quasi-static deformation, the dynamic effect can be shown, see

Fig. 13. From both Figures it is obvious that the dynamic effect is much larger towards the end of the side wall because the pressure wave has excited the mode of the structure with a similar wave length as the pressure pulse during its entire passing along the vehicle section. This leads to the largest amplifications if the propagation speed of the mode $v_{mode} = \lambda_{mode} f_{mode}$ and the relative velocity between the two vehicles agree. For the TR08, this speed v_{crit} is slightly lower than the maximal possible relative velocity between the two vehicles as shown in
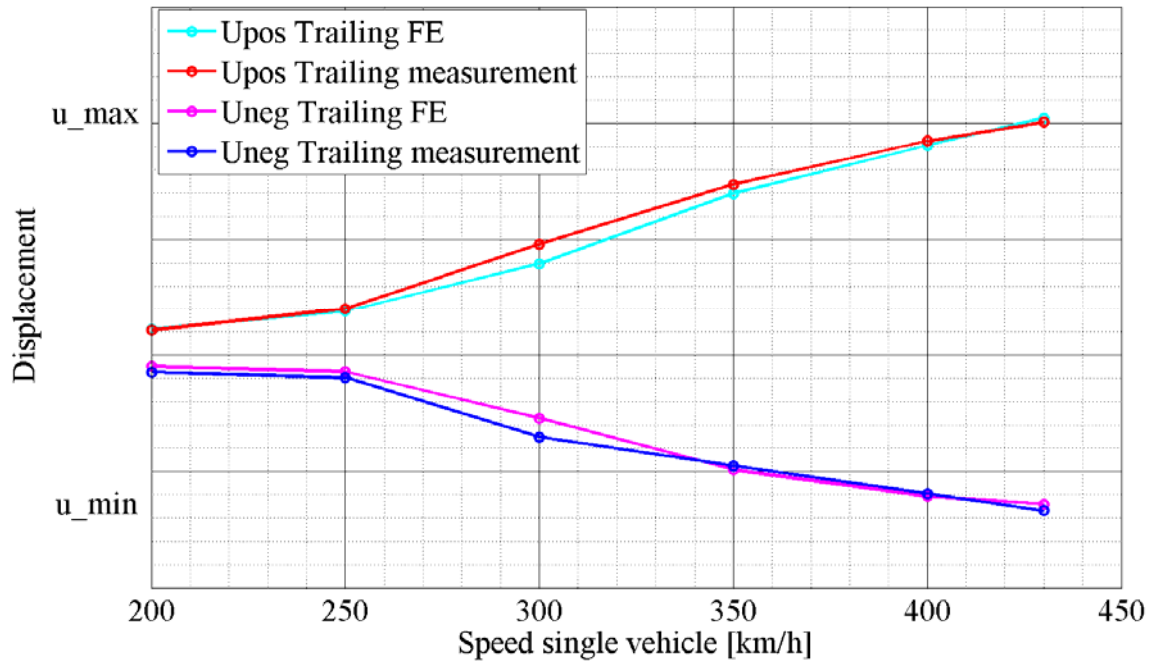
Fig. 13.

Fig. 11: Comparison between measurements and FE results. Deformation at the end of the carriage body
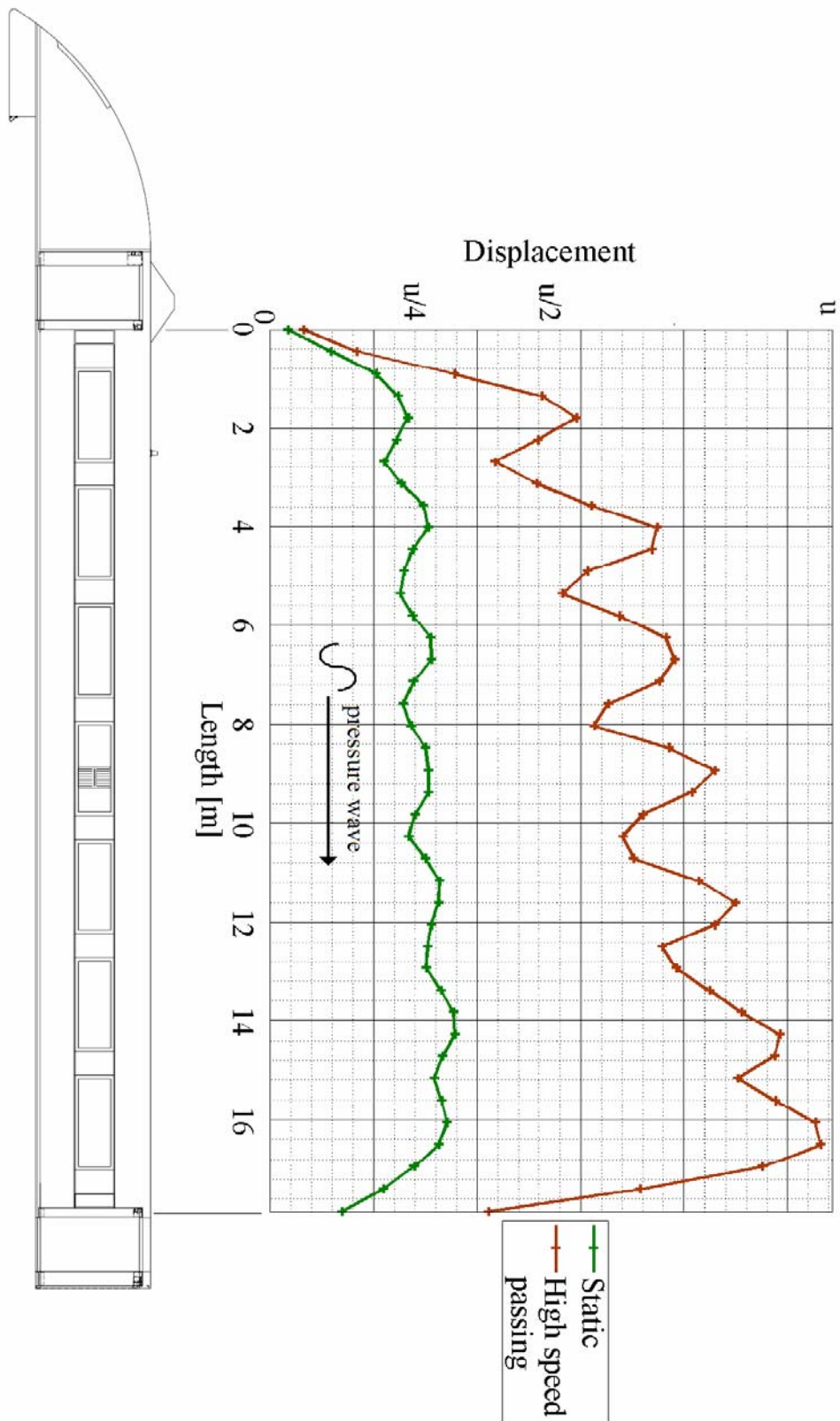
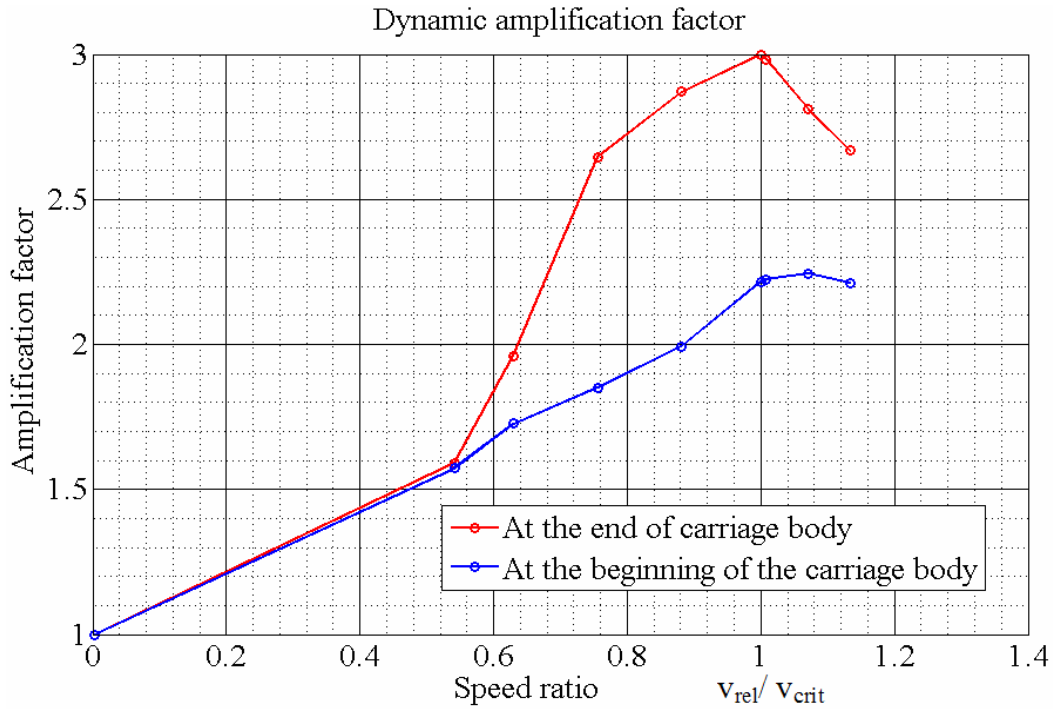**Fig. 12**: Deformation along the sidewall at high speed passing

Fig. 13: Dynamic amplification factor in relationship to the relative speed

5 RESULTS

The model is verified by a comparison with several measurements under the given operating conditions. The results show that the amplitudes of the structural deformation are largest at a specific relative velocity v_{crit}, which corresponds to the propagation speed of a global mode of the carriage body that possesses nearly the same wavelength as the pressure wave $\lambda_{mode} \approx \lambda_{p\_wave}$. As the amplitude increases with the propagation of the excitation along the side wall, it is largest towards the end of each carriage. In relation to the static displacement, it is possible to compute a dynamic amplification factor for the deformation. This factor is shown for the beginning and the end of the side wall of each vehicle section in Fig. 13. In this situation, the oncoming vehicle is always travelling at v_{max} = 430 km/h and a constant distance between the two tracks (therefore the pressure amplitude is constant), while the speed of the considered vehicle is varied.

From the figure it is obvious that the dynamic effect is much larger towards the end of the side wall because the pressure wave has excited the mode of the structure during its entire passing along the vehicle section. This leads to the largest amplifications if the propagation speed of the mode $v_{mode} = \lambda_{mode} f_{mode}$ and the relative velocity between the two vehicles agree. For the TR08, this speed v_{crit} is slightly lower than the maximal possible relative velocity between the two vehicles as shown in Fig. 13

The results are important for calculating the life time of the carriage structure depending on the operating conditions and to optimize the architecture of the carriage body. In summary, the mechanical load on the carriage body depends mainly on:

i)   the amplitude of the pressure wave, given by
- the velocity of the oncoming vehicle
- the bow-shape of the oncoming vehicle
- the distance between the two tracks

ii)   the relation between the propagation speed of the structural Eigenmode with the corresponding wavelength and the relative velocity between the two vehicles

iii)   the load at a specific point of the structure depends on its location within the carriage body, but not on the overall length of the vehicles or the position of the carriage body within the vehicle set.

Another fundamental result of the presented work is that the developed FE-modeling technique for the carriage body — using a combination of shell elements with layered 3D elements — has clear advantages over conventional models using either 2D shell or traditional volume elements only. This technique can be applied to other high-speed rail vehicles with similar carriage cells. Such allowing a transient analysis of thin side walls with large surfaces consisting of profiles and/or sandwich structures.

REFERENCES

[1]   H. Lobach, G. Köb. Transrapid vehicles for Shanghai. In: Rausch et al. [5], 56–69, 2003.

[2]   Holmes, B. S., and Schroeder, M. P., "High-Speed Passenger Train Aerodynamic Loading Effects on Passing Trains", U.S. DOT Federal Railroad Administration report, DOT/FRA/ORD01-xx, April 2001.

[3]   S. Monaco. Structural Vibrations of the Carriage Body Cell caused by dynamic Pressure Load. Master Thesis. Politecnico di Milano, Dipartimento di Meccanica, December, 2007.

[4]   J.L. Peters. Aerodynamics of very high speed trains and maglev vehicles: State of the art and future potential. *Int. Journal of Vehicle Design*. Special Publication SP 3: Impact of Aerodynamics on Vehicle Design, 308–341, 1983.

[5]   K.F. Rausch, K. Rießberger, H. Schaber (eds.). Special edition Transrapid. *ZEVrail, Glasers Annalen*. **127**, 2003.

[6]   R. Schach, P. Jehle, R. Naumann. *Transrapid und Rad--Schiene—Hochgeschwindigkeitsbahn*. Springer, Berlin 2006.

[7]   Th. Tielkes. Aerodynamic Aspects of Maglev Systems, Proceedings of the 19th International Conference on Magnetically Levitated Systems and Linear Drives, Maglev 2006. Edited by R. Schach and M.Witt, 641–649. Institute of Construction Management, TU Dresden, Germany, 2006.

[8]   F. Dignath, Q. Zheng. Transrapid Vehicles: Effects of Aerodynamics on the Internal Pressure and the Structure of the Carriage Body. Proceedings of the 8th World Congress on Railway Research, May 18th-22nd, 2008, Seoul, Korea.